Journal of Physical & Chemical Research

Journal homepage: https://ojs.univ-bba.dz

Angular and energy dispersion in neutron-rich nuclei by neutron evaporation: A Monte Carlo simulation

Khalfallah Farid[1,2*], **Chia Leila**[1]

[1] *Department of matter science, Faculty of sciences and technology, University of Mohamed El Bachir El Ibrahimi, Bordj Bou Arreridj, 34030 Algeria*
[2]*Laboratory of Materials Physics, Radiation and Nanostructures (LPMRN), Faculty of Sciences and Technology, Mohamed El Bachir El Ibrahimi University, Bordj-Bou-Arreridj 34030, Algeria.*

* *E-mail address: f.khalfallah@univ-bba.dz*
DOI: https://doi.org/10.58452/jpcr.v1i2.20

Article history
Received March 20, 2022
Accepted for publication June 02, 2022

Abstract

In this paper we present the results of a Monte Carlo simulation of the effects of neutron evaporation on the angular and energy dispersions in neutron-rich nuclei as a function of the mass number *A*, the kinetic energy *E* and the number of emitted neutrons. We based our simulation on the assumption of an isotropic random distribution for the neutron emission angles in space and on a Maxwell-Boltzmann distribution for the kinetic energy of the evaporated neutrons. Our results confirm large angular and energy dispersions for light, low-energy nuclei and for high neutron channels.

Keywords: Energy and angular dispersion, fusion reaction, neutron evaporation, neutron rich nuclei, Monte Carlo.

1. Introduction

The emission or evaporation of neutrons in unstable neutron-rich nuclei following fusion-evaporation reactions is a common phenomenon in nuclear reaction physics. This process allows the compound nucleus to lose a significant portion of its excitation energy by evaporating its excess of neutrons during its flight toward the detector. These neutron emissions can have significant effects on the trajectory and kinetic energy of the emitting nucleus and thus affecting the detection efficiency in nuclear detection systems like magnetic separators [1-3]. It can also affect the precision measurements of the implantation energy for focal plane detectors [4].

In this work, we perform a Monte Carlo calculation of the angular and energy effects of neutron evaporation on the residual nucleus. In the field of fusion-evaporation and fission reactions, several Monte Carlo simulations for statistical neutron evaporation and fission fragments has been made notably by Vanderbosh & all [5] and Kawano & al. [6-7]. Recently the field has gained a great interest because of its importance in the fusion of heavy and super-heavy elements [8]. Our calculations consist of a systematic study of neutron's angular and energy dispersion depending on two parameters, the masse number *A* of the nucleus (from relatively light to heavy nuclei) and the neutron emission channel (from *1n* to *5n*). The simulations were carried out using CERN Fortran libraries specialized in the generation of random numbers.

2. Method

The emission of each neutron from the nucleus contributes to the deviation of the trajectory of the evaporation residue as well as to the dispersion of its kinetic energy. Due to the conservation of momentum, one can expect maximum angular deviation of the nucleus when the neutron is emitted in a direction perpendicular to the axis of motion, while if it is emitted in a parallel direction, the deflection will be minimal. For the kinetic energy of the emitting nucleus, It is the opposite that is expected. Parallel neutron emissions contribute to a maximum variation of the energy of the nucleus resulting in a decreasing kinetic energy for a forward emission and an increasing energy for a backward emission. A minimal energy variation occurs if the neutrons are emitted perpendicularly.

In order to evaluate the importance of these two phenomena we perform our Monte Carlo simulation based on two assumptions: First, we suppose an isotropic random distribution of neutron emission angles in space. Second, we consider that each neutron is emitted with a kinetic energy distributed according to a statistical evaporation model of Maxwell-Boltzmann type.

2.1 Angular and energy dispersion

To calculate the deflection angle $\boldsymbol{\theta}$ of the residual nucleus and its kinetic energy $\boldsymbol{E}$ after the emission of several neutrons, we start by writing the kinematic equations representing the movement of the nucleus before and after the emission of a first neutron. Suppose that we have a neutron-rich nucleus Y (figure 1) in an excited state with mass $\boldsymbol{M_Y}$, excitation energy $\boldsymbol{E^*}$, momentum $\boldsymbol{P(Y)}$ and a kinetic energy $\boldsymbol{T_Y}$. The evaporation of the first neutron with kinetic energy $\boldsymbol{T_n}$ occurs through the reaction:

$$ {}^{A}_{Z}Y_N \rightarrow {}^{A-1}_{Z}Y'_{N-1} + 1n \tag{1} $$

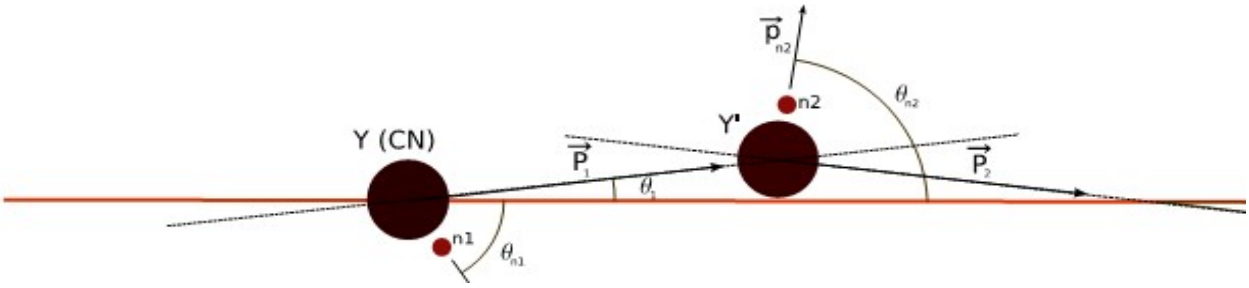

Figure 1. Schematization of the angular deviations of the residual nucleus after the emission of two neutrons.

Conservation of energy and momentum allow us to calculate the energy and momentum of the residual nucleus and of the evaporated neutron.

2.1.1 Conservation of energy and momentum

The application of the principles of momentum and energy conservation on the reaction (1) leads to the following equations for the excitation energy and momentum of the nucleus before and after emission of the first neutron (channel 1n):

$$ \vec{P}(Y) = \vec{P}(Y') + \vec{P_n} \tag{2} $$

$$E'^{*} = E^{*} - (T_{Y'} - T_Y) - (T_n + S_n) \tag{3}$$

Where

$$S_n = (M_{Y'} - M_Y + M_n)c^2 \tag{4}$$

is the bending energy of the neutron. The kinetic energy $\boldsymbol{T_n}$ of the emitted neutron will be derived from a Maxwell-Boltzmann distribution.

2.1.2 Energy distribution of evaporated neutrons

For our calculation, the energy profile used for the evaporated neutrons is a well known model in statistical physics and neutron physics. It is the model of a neutron gas according to a Maxwell-Boltzmann statistics. In this model, the energy distribution function of the evaporated neutrons is given by a Maxwell-Boltzmann function:

$$f(T_n) = \frac{\sqrt{T_n}}{T^2} e^{-\frac{T_n}{kT}} \tag{5}$$

Where:

$$\boldsymbol{kT \sim \frac{E^{*}}{\sqrt{A/8}}}$$

is the temperature of the nucleus which is proportional to its excitation energy.

2.1.3 Recurrence relations for angular deviation and energy

For the subsequent neutron emissions (2n, 3n... 5n channels), using the same principles at every step of a second neutron evaporation we can derive the following recurrence relations between the excitation energy of the residue, its momentum and the neutron energy before and after the emission of the k-*th* neutron.

$$\overrightarrow{P_{k+1}} = \overrightarrow{P_k} - \overrightarrow{P_{n,k}} \tag{6}$$

$$E^{*}_{k+1} = E^{*}_k + (T_k - T_{k+1}) - (T_n + S_{nk} \tag{7}$$

$$S_{nk} = (My_{k+1} + M_n - M_{Y_k})c^2 \tag{8}$$

In spherical coordinates, where the z axis is the direction of the movement of the nucleus, if $\boldsymbol{\theta_k}$ and $\boldsymbol{\varphi_k}$, $\boldsymbol{\varphi_{k+1}}$ and $\boldsymbol{\theta_{k+1}}$ are the angular coordinates of the nucleus before and after emission of the k-*th* neutron then we have:

$$\begin{cases} P_{k+1}\sin\theta_{k+1}\cos\varphi_{k+1} = P_k\sin\theta_k\cos\varphi_k - p_{nk}\sin\theta_{nk}\cos\varphi_{nk} = f_{xk} \\ P_{k+1}\sin\theta_{k+1}\sin\varphi_{k+1} = P_k\sin\theta_k\sin\varphi_k - p_{nk}\sin\theta_{nk}\sin\varphi_{nk} = f_{yk} \\ P_{k+1}\cos\theta_{k+1} = P_k\cos\theta_k - p_{nk}\cos\theta_{nk} = f_{zk} \end{cases} \tag{9}$$

The right hand side of these equations are functions of the angular and momentum variables at the *k*-step and are labelled: $\boldsymbol{f_{xk}}$, $\boldsymbol{f_{yk}}$, $\boldsymbol{f_{zk}}$.

Using these functions we finally obtain the energies and angular variables of the evaporation residue at the (*k+1*)-step :

$$\begin{cases} T_{k+1} = \frac{P_{k+1}^2}{2M_{Y_{k+1}}} = \frac{f_{xk}^2+f_{yk}^2+f_{zk}^2}{2M_{Y_{k+1}}} \\ cos\theta_{k+1} = \frac{f_{zk}}{\sqrt{f_{xk}^2+f_{yk}^2+f_{zk}^2}} \\ \cos\varphi_{k+1} = \frac{f_{xk}}{\sqrt{f_{xk}^2+f_{yk}^2}} \end{cases} \quad (10)$$

2.2 Monte-Carlo simulation

The Monte Carlo method [9-10] is used in our simulation, it is a stochastic method that allow us to introduce the randomness inherent to this type of nuclear interactions. The calculation of the energies and angles at each neutron emission is performed from the recurrence relations (9) and (10), the angle of deviation of the evaporation residues θ_{k+1} represents the deviation of the nuclei with respect to the initial axis of trajectory after evaporation of k neutrons.

The emission of neutrons can occur randomly in any direction in space, to obtain an isotropic distribution of the direction of emission, we use a uniform random numbers generator. Therefore, at each iteration, the azimuth angle φ_{nk} is generated uniformly between 0 and 2π and the cosine of the angle θ_{nk} is generated uniformly between -1 and 1. The neutrons momenta are deduced from their energies. As mentioned above, the statistical evaporation of neutrons follows a Maxwell-Boltzmann distribution, thus the neutron energies are generated according to this distribution. The random number generators used in our calculations are part of the CERN Fortran library.

3. Results

The Monte-Carlo simulation was performed for a wide range of the mass A of the nuclei from A= 40 (light nuclei) to A=260 (heavy nuclei) with a 20-units step.

For each value of A, we simulated a number of 20000 nuclei and for each nucleus the five channels 1n, 2n, 3n, 4n and 5n (cold and hot fusion) where considered. All the calculations were made for 2 values of the initial kinetic energy of the emitting nucleus: E=10MeV and E=50MeV. For the initial excitation energies E* of the nuclei, we worked with two values, E*=30MeV for the nuclei with initial kinetic energy E=10MeV and E*=60MeV for the more the energetic nuclei with initial energy of 50 MeV.

The result of the simulation is presented in the figures below plotted in the form of histograms for light (A=40, 60, 80) and heavy (A=220, 240, 260) nuclei. The angular and energy distribution of the evaporation residue are shown for the 3n channel only with a polynomial fit for the angular part and a Gaussian fit for the energy part (red lines). Similar distributions were obtained for the other 1n, 2n, 4n and 5n channels.

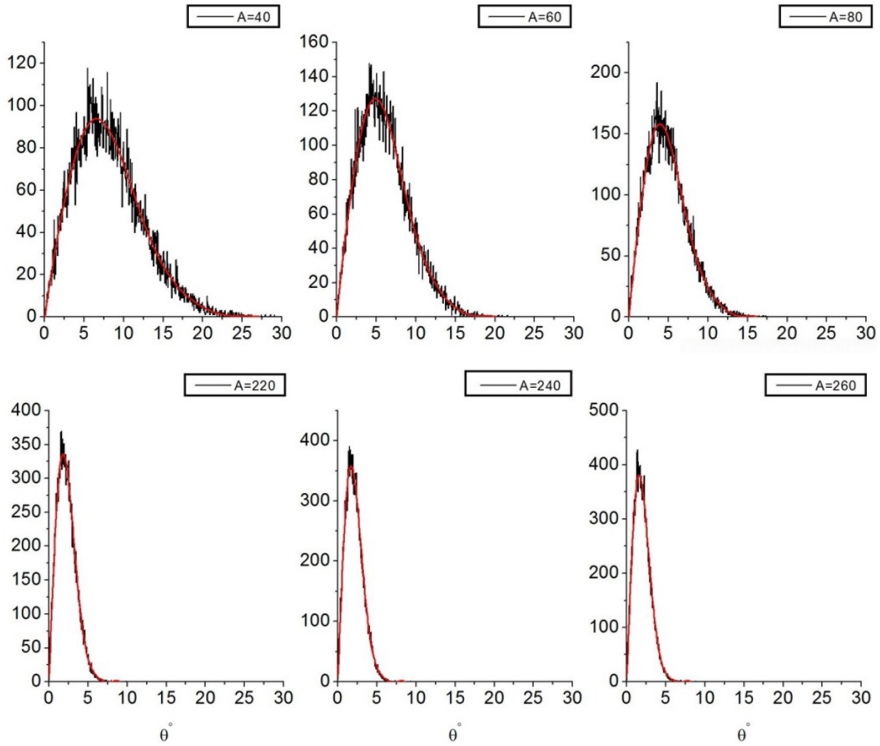

Figure 2. Angular distribution of the evaporation residue for E=10MeV - 3n channel

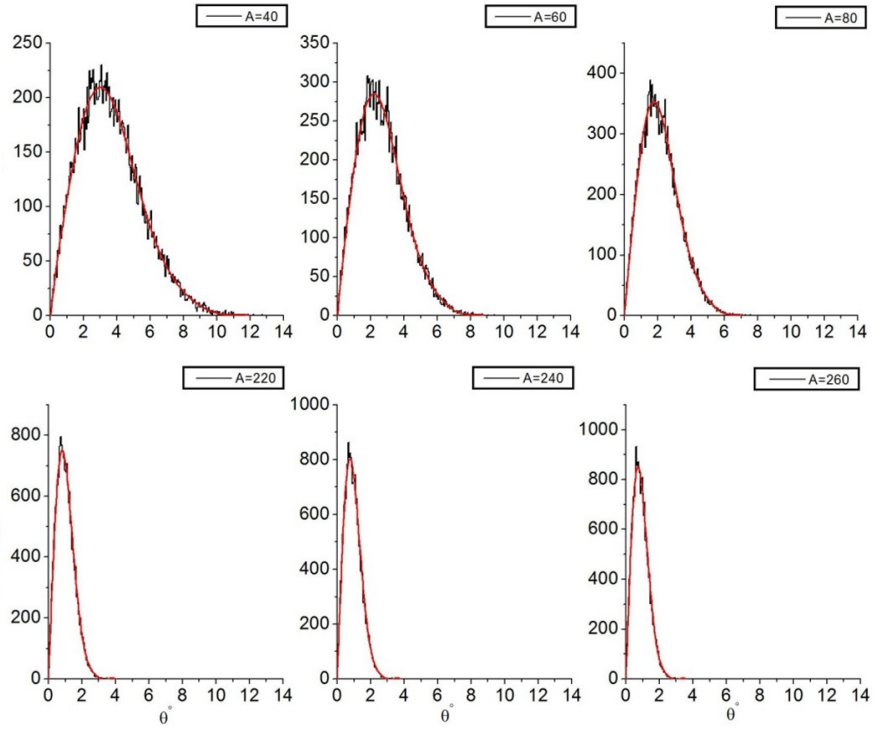

Figure 3. Angular distribution of the evaporation residue for E=50MeV - 3n channel

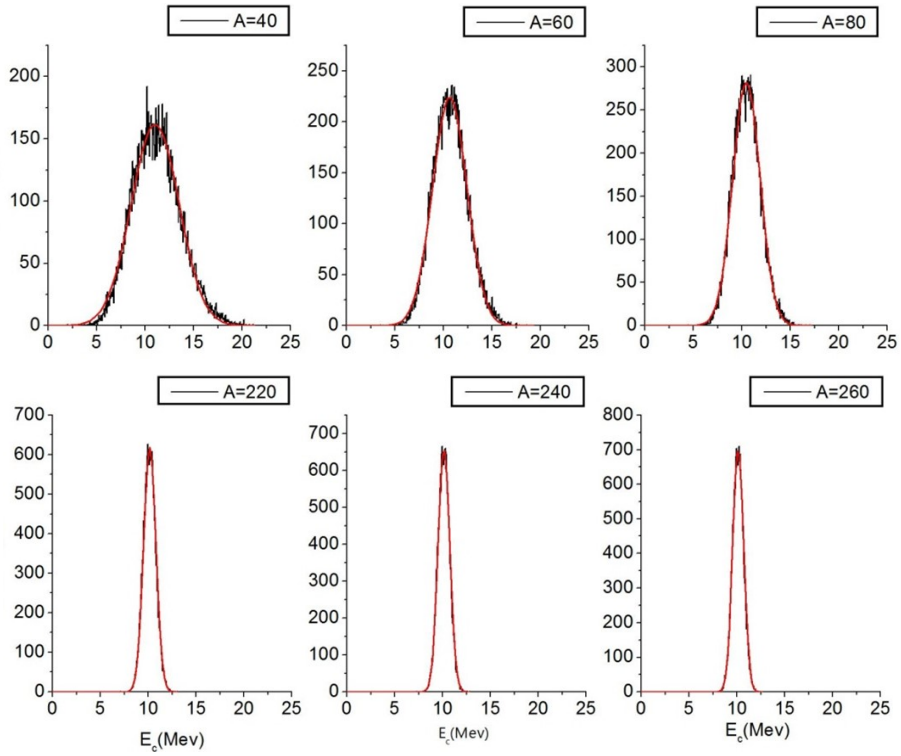

Figure 4. Energy distribution of the evaporation residue for E=10MeV - 3n channel

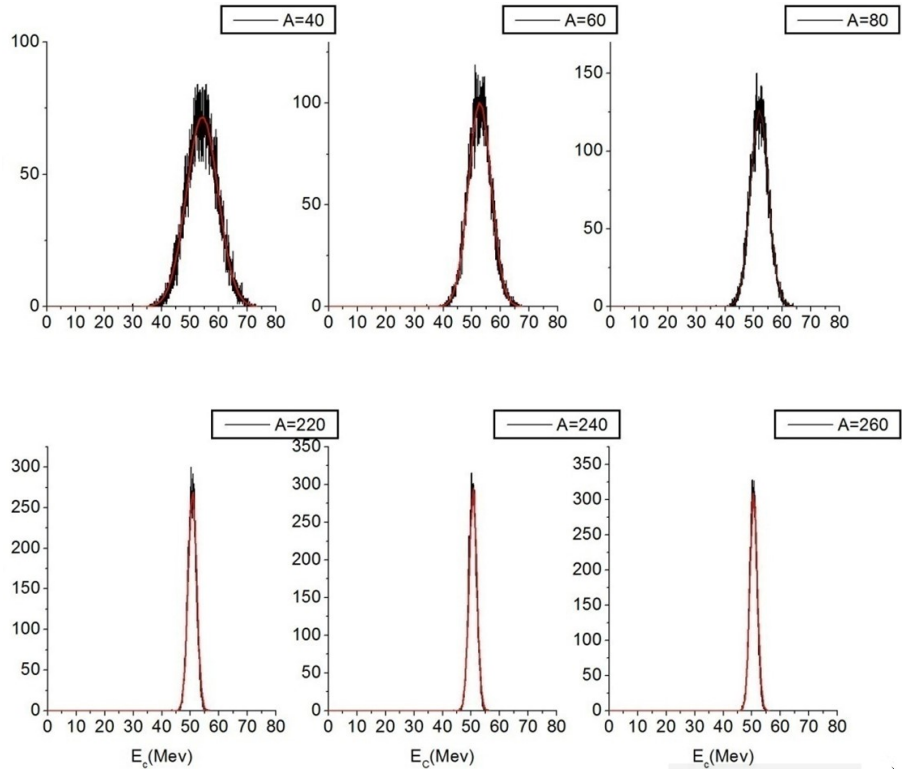

Figure 5. Energy distribution of the evaporation residue for E=50MeV - 3n channel

From the figures of the angular distributions (figures 2 & 3) we clearly see that the vast majority of the residue (after 3 neutrons evaporation) are concentrated in a region around a maximum angle θ_{max}. We observed the same behaviour for the other channels. The nuclei are concentrated in a crown around the axis of movement and the central region corresponding to the axis of motion (θ=0) is almost empty of nuclei. We also observe that the distributions are wider for light nuclei and become narrower with increasing mass number A.

For the energy spectra (figures 4 & 5), we observe normal (Gaussian) distributions with a decreasing widths FWHM (Full Weight Half Maximum). The widths are larger for light nuclei and decrease with increasing nucleus mass. One also notices a light shift of the average value of the energy (the center of the normal curve) compared to its initial values.

In order to examine more closely the influence of the number of neutrons emitted as a function of the mass of the nuclei A and make a comparison between the two cases of low (E=10MeV) and high (E=50Mev) initial energy we extracted the maximum values of the angular dispersion θ_{max} (the dominant angle of deviation). On the other hand, to evaluate the importance of the energy dispersion, we also extracted the widths of the energy spectra FWHM.

These values are shown in the following tables and the corresponding plots are presented below.

Table 1. Dominant angular dispersion θ_{max} (in degree) for E=10MeV

Channel	A=60	A=100	A=140	A=180	A=220	A=260
1n	2.318	1.550	1.203	1.010	0.875	0.754
2n	3.302	2.303	1.819	1.499	1.298	1.146
3n	4.921	3.299	2.585	2.156	1.806	1.594
4n	5.778	3.951	2.961	2.442	2.110	1.892
5n	6.128	4.413	3.399	2.815	2.427	2.128

Table 2. Dominant angular dispersion θ_{max} (in degree) for E=50MeV

Channel	A=60	A=100	A=140	A=180	A=220	A=260
1n	1.022	0.694	0.532	0.454	0.380	0.339
2n	1.463	1.017	0.797	0.661	0.571	0.488
3n	2.385	1.498	1.139	0.943	0.839	0.707
4n	2.518	1.760	1.344	1.118	1.000	0.836
5n	2.653	1.897	1.484	1.237	1.071	0.938

Table 3. Energy distribution width FWHM (in MeV) for E=10MeV

Channel	A=60	A=100	A=140	A=180	A=220	A=260
1n	1.652	1.119	0.868	0.718	0.617	0.544
2n	2.392	1.604	1.239	1.024	0.879	0.774
3n	3.552	2.375	1.830	1.509	1.294	1.139
4n	4.186	2.753	2.107	1.741	1.487	1.308
5n	4.649	3.160	2.422	1.978	1.702	1.496

Table 4. Energy distribution width FWHM (in MeV) for E=50MeV

Channel	A=60	A=100	A=140	A=180	A=220	A=260
1n	3.695	2.503	1.938	1.603	1.378	1.215
2n	5.345	3.605	2.776	2.295	1.968	1.736
3n	7.948	5.310	4.089	3.371	2.890	2.545
4n	9.161	6.160	4.717	3.892	3.325	2.926
5n	9.792	7.047	5.373	4.360	3.785	3.310

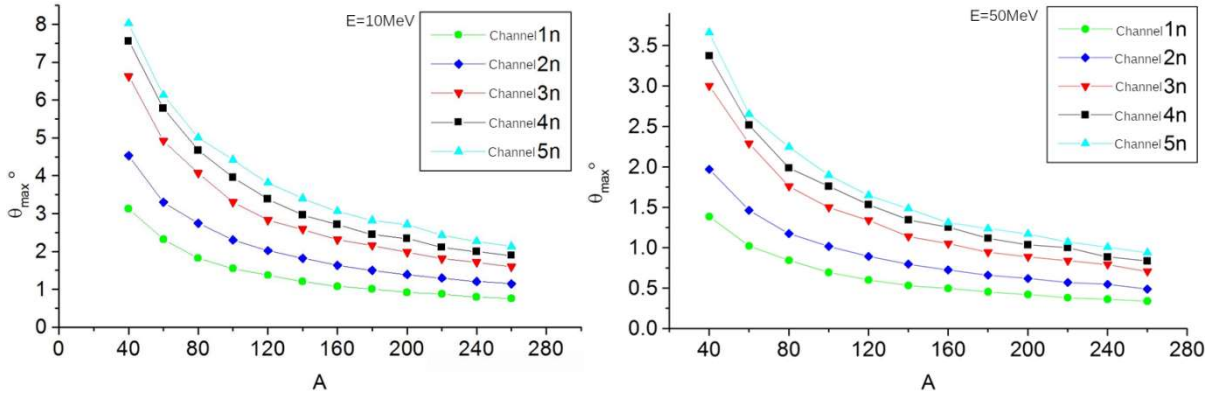

Figure 6. Dominant angular dispersion θ_{max} (all 5 channels) for E=10MeV and E=50MeV

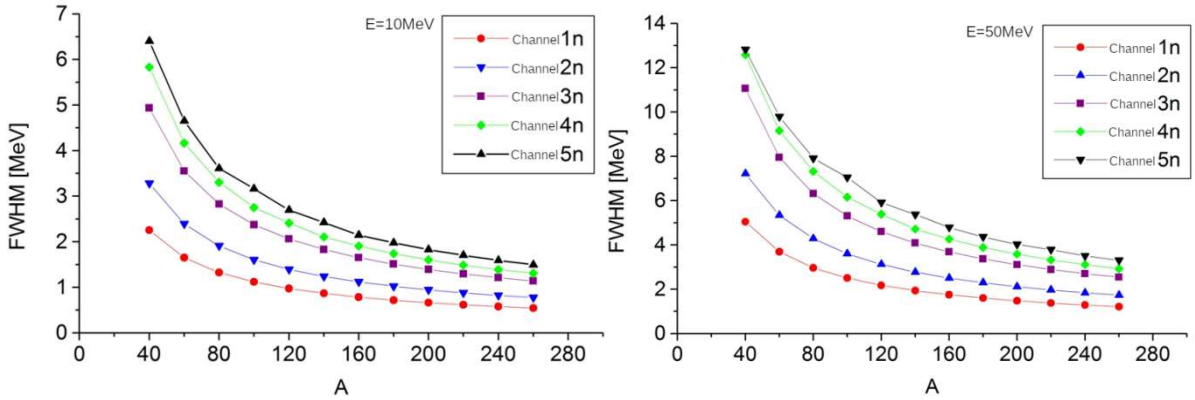

Figure 7. Energy distribution widths FWHM (all 5 channels) for E=10MeV and E=50MeV

4. Discussion

The Monte Carlo simulation shows that the angular dispersion of the residual nuclei, given by θ_{max} (figures 6), has the same decreasing tendency with increasing mass number A for all channels independently of the initial energy of the nucleus.. This observation was predictable since a heavy nucleus has more inertia and momentum (at equal energies) than a light one and is therefore more difficult to deflect by neutron emission. We notice that the decrease is however more pronounced for the high neutron channel. We also observe that θ_{max} increases with the number of neutrons emitted independently of the mass of the nucleus and its initial energy. This increase is more visible for light nuclei. At last, by comparing curves from E=10MeV and E=50MeV, it can be seen that the angular deviations are less important for E=50MeV. This observation was also expected since the more energetic nuclei are more difficult to deflect. These results are in agreement with measurements in experimental detection systems.

For the case of the energy dispersion estimated by the distribution's width FWHM, figures 7 shows a predictable decrease with mass number A for all channels and for the two initial energy values. However, the decreases are greater for multiple neutron emission. We also observe that the widths are wider for E=10MeV (up to 6.4MeV) in comparison with that corresponding to E=50MeV (up to 12.8MeV) independently of the number of neutrons emitted.

5. Conclusion

Our Monte Carlo calculations led to several results, the most important is the fact that the emission of neutrons has the effect of deflecting the majority of the emitting nuclei inside a corona with a wider angle for light and low energy nuclei and for high neutron channels. These deviations can reach up to 8° for the 4n and 5n channels in light nuclei and must be taken into account in the estimation of the efficiency of detection systems. On the other hand, it has been found that the energy dispersion of nuclei is greater for light and low-energy nuclei in the 4n and 5n emission channels, it can reach 3.2MeV for light nuclei having low energies of 10MeV and will therefore have a significant influence on the energy measurements in focal plane detectors.

References

[1] J. Uusitalo & al, Nuclear Instruments and Methods in Physics Research B, v. 204, 638-643 (2003)
[2] I.H. Lazarus & al., IEEE Trans. Nucl. Sci. 48, 567 (2001)
[3] H. Savajols, Nuc. Phys. A 654, 1027 -1032 (1999)
[4] R. D. Page et al, Nuclear Instruments and Methods in Physics Research B, v. 204, 634-637 (2003)
[5] R.Vandenbosch & al., Nuc. Phys. 25 511-521 (1961)
[6] T. Kawano & al., EPJ Web of Conferences 21, 04001 (2012)
[7] T. Kawano & al., Nuc. Phys. A 913, 51-70 (2013)
[8] P. Armbruster, Annual Review of Nuclear and Particle Science 50, 411-479 (2000)
[9] M. H .Kalos, W. A. Paula. Monte Carlo Methods, WILEY-VCH, (2008)
[10] P.R.Cheistian, C.George, Méthodes de Monte Carlo avec R, Springer-Verlag, France (2011).